Environ Earth Sci (2011) 63:1447–1461
DOI 10.1007/s12665-010-0743-8

SPECIAL ISSUE

A comparison of the properties and salt weathering susceptibility of natural and reconstituted stones of the Orval Abbey (Belgium)

C. Thomachot-Schneider · M. Gommeaux · G. Fronteau · C. T. Oguchi · S. Eyssautier · B. Kartheuser

Received: 1 July 2010 / Accepted: 11 September 2010 / Published online: 26 September 2010

Abstract The Orval Abbey, a major monument of southern Wallonia, Belgium, was partly destroyed and rebuilt several times between the Middle Ages and the present time. The oldest parts are made of natural stones of local origin (Bajocian and Sinemurian limestones) and the most recent parts are mostly made of reconstituted stone. The process of reconstituted stone making is not known. Although confronting the same environmental conditions, the reconstituted stone is much more susceptible to weathering than the natural limestones, especially to salt crystallisation. The present study compared the mineralogical and petrophysical properties of these building materials to gather information on the making of the reconstituted stone and to understand the difference in salt susceptibility between natural and reconstituted stones. Microscopic observations and petrophysical measurements showed that the reconstituted stone is composed of debris of Sinemurian and Bajocian limestone and cement, and the salt efflorescences were thenardite. Within the cement, amorphous grains were found that may correspond to grains of clinker, which have not reacted during stone making. Although its porosity and water transfer properties were close to that of the Bajocian limestone, its pore access distribution was centred around 0.1 μm. Furthermore, the details of the pore size distribution allowed calculating salt susceptibility indices that were very high in the case of the reconstituted stone. Thus, the composition of the cement and the pore size distribution are likely the two factors explaining a high susceptibility of the reconstituted stone to salt weathering.

Keywords Reconstituted stone · Bajocian and sinemurian limestone · Salt weathering · Thenardite · Heritage conservation

C. Thomachot-Schneider (✉) · M. Gommeaux · G. Fronteau · S. Eyssautier
Groupe d'Étude sur les Géomatériaux et les Environments Naturels, Anthropiques et Archéologiques EA3795 (GEGENA), Université de Reims Champagne-Ardenne, 2 Esplanade Roland Garros, 51100 Reims, France
e-mail: celine.schneider@univ-reims.fr

C. T. Oguchi
Geosphere Research Institute (GRIS), Saitama University, 255 Shimo-Okubo, Sakura-ku, Saitama 338-8570, Japan

B. Kartheuser
CEntre de Ressources TEchnologiques en CHimie (Certech), Rue Jules Bordet, Zone Industrielle C, 7180 Seneffe, Belgium

Introduction

The choice of the materials for the building of monuments is generally a compromise between technical and economical constraints. Both the technical and economical factors are subject to change over time, especially when several phases of building, destruction, rebuilding and conservation works alternate over long periods (Gomez-Heras et al. 2010; Rozenbaum et al. 2008). Thus, some monuments, in their present state, comprise different parts of different ages that are made of different materials. Those different parts are submitted to weathering, varying in type and intensity. Current conservation strategies have to deal with this mosaic pattern.

The Orval Abbey, a major monument in Wallonia, is a typical example of a monument with a long and polyphasic history. This monastery, currently affiliated to the Cistercian order, was first established in the twelfth century. The abbey is located over Sinemurian limestone formation (Lower Jurassic, ca. 200 Ma, LUX Fig. 1), also called

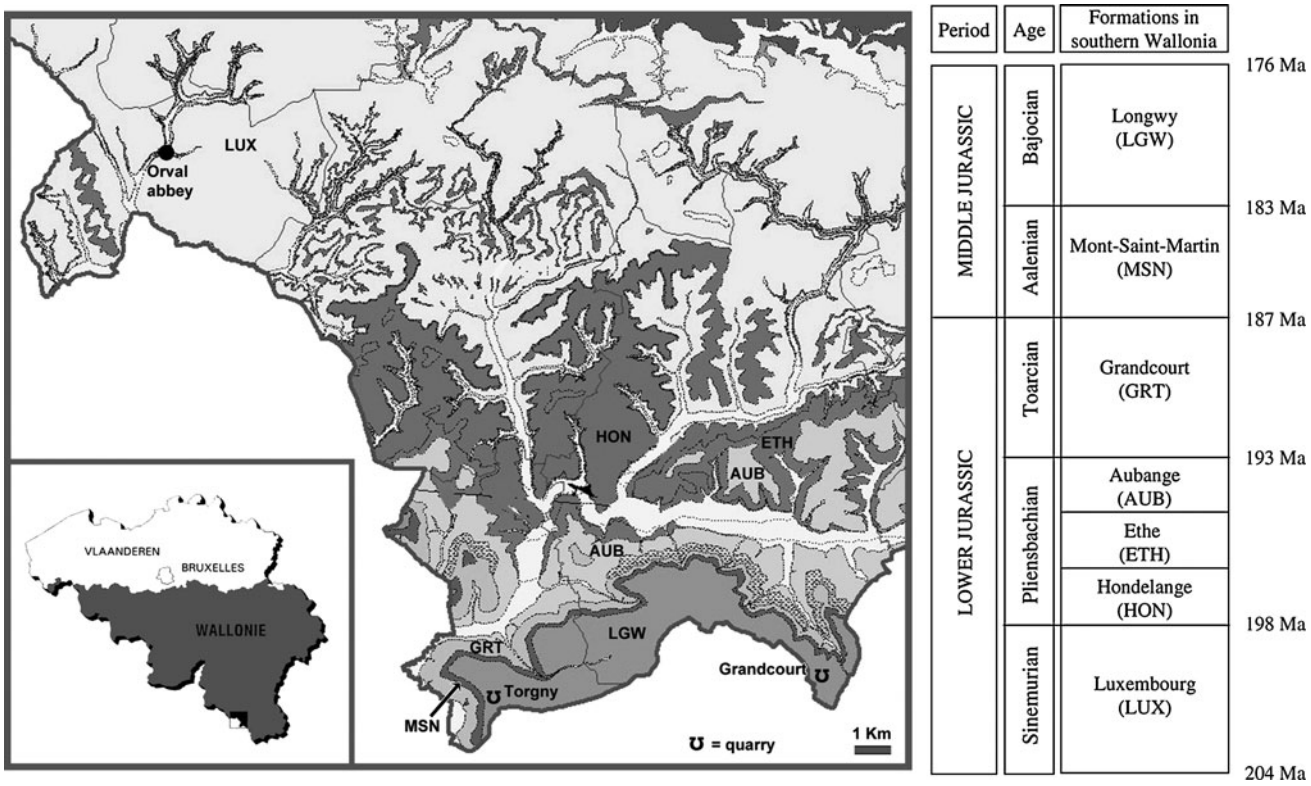

Fig. 1 Location of Orval Abbey on the geological map of South of Wallonia

Luxembourg formation. The mediaeval abbey is, however, partly built of this local stone and of Bajocian limestone (Lower Jurassic, ca. 180 Ma). Outcrops of this stone appear 20 km southeast of Orval (the Longwy formation, or LGW) and are spread over the France–Belgium border. They are still exploited nowadays and are known as "Pierre de Grandcourt" or "Torgny" on the Belgian side and "Pierre de Jaumont" on the French side (Brigaud et al. 2009a, b).

The Orval Abbey was destroyed in 1637 during the French–Spanish war by the French army. The mediaeval abbey was subsequently restored and a new abbey was built next to it during the eighteenth century. The site was destroyed again by the French insurgents in 1793 during the French Revolution. It remained in a state of ruin until 1926, when the Cistercian order re-established a monk community. At that time, the community undertook clearing the ruins away and started building a new abbey. The mediaeval ruins were kept mostly untouched (Fig. 2a). The remains of the eighteenth-century abbey were totally removed, except the foundations to allow the rebuilding of the modern abbey over them (Sarlet and Matthys 1995).

Owing to the extent of the works, it was necessary to survey the possible stone supplies around the abbey. The community initially secured a supply of 6,000 m^3 of premium quality Bajocian limestone, from a quarry located about 30 km southeast of the abbey (Pas-Bayard quarry). The works also employed Sinemurian stone from local

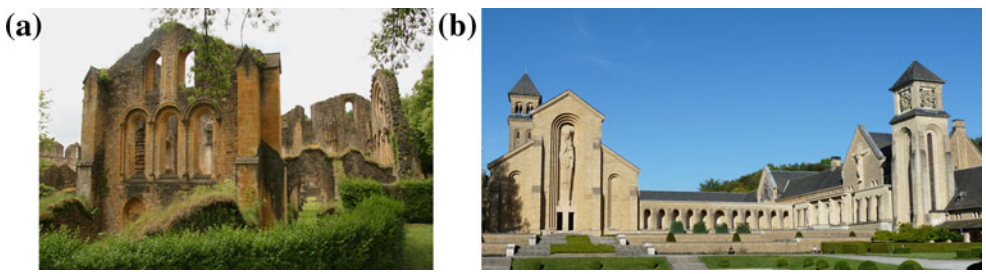

Fig. 2 Overview of the Orval Abbey: **a** sample view of the ruins of the mediaeval abbey, built of Bajocian limestone (Pierre de Grandcourt, Longwy formation). Apart from consolidation works (visible, for example, at the sides of the wall in the foreground), the ruins were cleared away in the early twentieth century, but mostly untouched. **b** Modern part, mostly built of artificial reconstituted stone

quarries and of lower quality wherever possible. Due to high prices and limited availability of stone, it became necessary to investigate the possibility to reuse debris removed from the ruins and wastes of natural freestone cutting. To this purpose, reconstituted stone was produced locally and used as freestone. The production of reconstituted stone spanned from 1932 to the completion of the new abbey in 1948 (Fig. 2b).

In its current form, the Orval Abbey thus comprises parts made of Sinemurian and/or Bajocian natural stone and parts made of reconstituted stone. Though the natural and reconstituted materials are quite similar in aspect and composition (Fig. 3a), their susceptibility to weathering is quite different. On the modern monument built with reconstituted stone, the growth of moist areas, salt efflorescence, powdering and flaking of the surface in the capillary zones (Fig. 3b, c) and the cracking of blocks due to frost action have been observed (Fig. 4). These weathering patterns are not particularly observed on parts of the monument built with natural limestones, such as the Bajocian or the Sinemurian one, on which only biological colonisation was observed.

Salt damages depend on (1) the porous network of the stone, (2) the type of salts and their amount and (Ruiz-Agudo et al. 2007) (3) the climatic conditions, especially the wetting–drying cycles (Goudie and Parker 1998). The porous network controls capillary and drying kinetics and mechanical strength (Yu and Oguchi 2009; Mosquera et al. 2006; Benavente et al. 2007) while cement composition can release salts over time, especially sodium and calcium sulfates (Rodriguez-Navarro and Doehne 1999).

Different susceptibilities to weathering of natural and reconstituted stones of the Orval Abbey could be explained by change in the porous network of both materials and/or

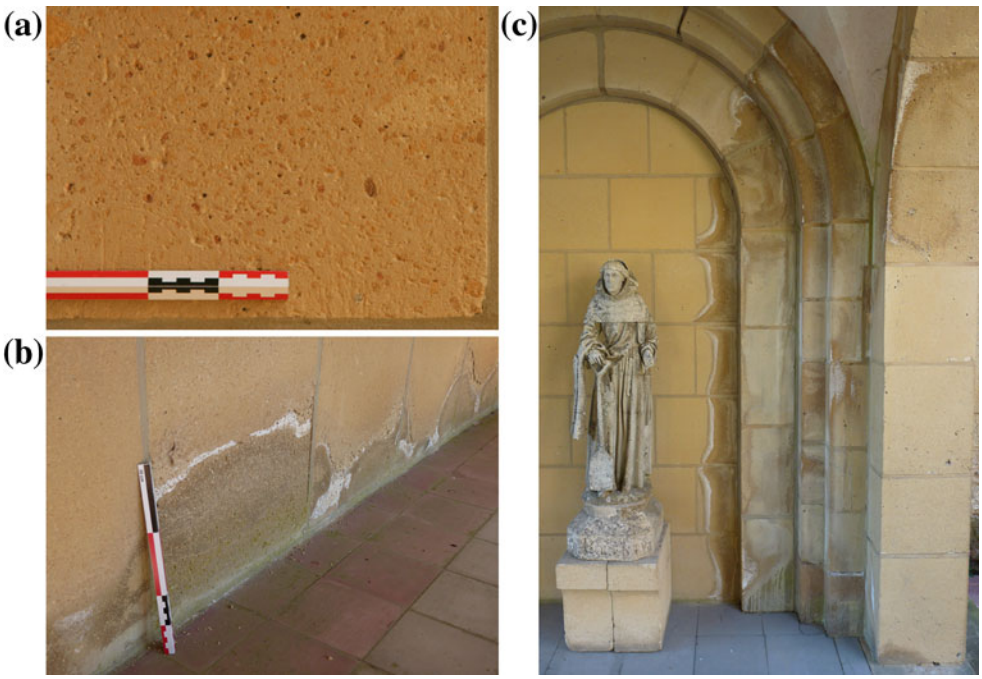

Fig. 3 Weathering patterns of the reconstituted stone. **a** Example of reconstituted stone; **b**, **c** efflorescences, flaking and moist area due to salt crystallisation in capillary zones

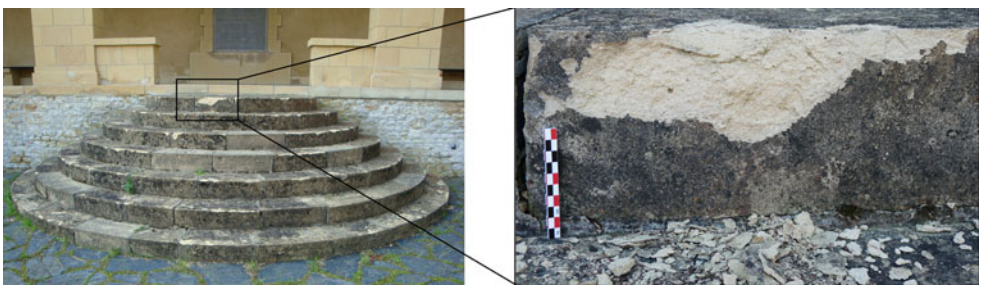

Fig. 4 Typical patterns of frost damage on reconstituted stone viewed on the stairs of the cemetery: cracking and chipping of blocks

composition of binders used for making the reconstituted stones.

Materials and methods

Climate in Orval

The climate in this part of Belgium is temperate. Minimum and maximum of precipitation occur, respectively, in April (59 mm) and December (83 mm) with 873 mm annual rainfall. Minimum and maximum of temperature occur, respectively, in January (0.6°C) and July (16.8°C) with 8.7°C annual average temperature (data from Virton weather station, Institut Royal Météorologique de Belgique, IRM).

Building materials of Orval

A quick survey of the abbey and of bibliographic information provided evidence that three main materials were used over the history of the monument: (1) the original Sinemurian limestone that constitutes the geological substratum in Orval (Luxembourg formation); (2) the original Bajocian limestone mainly used for the building of the abbey (Longwy formation); and (3) blocks of reconstituted stones used for building the modern part of the abbey. The Sinemurian limestone was sampled from outcrops due to building works in the immediate vicinity of the abbey. Blocks of the Bajocian limestone and the reconstituted stone were collected in the abbey's stone repository.

They were first subjected to mineralogical, chemical and physical analyses including X-ray diffraction, X-ray fluorescence, optical scanning electronic microscope (SEM) on rock samples and blue-coloured thin sections, water and mercury total porosity and capillary absorption.

Salt efflorescences were also sampled in walls of different places of the modern part of the abbey built of reconstituted stone.

Petrography

Colorimetry

Colour measurements were performed using a Chromameter CR-400 Konica-Minolta colorimeter with a light projection tube CR-A33c of 11 mm diameter. The illuminating system uses a pulsed xenon lamp, which provided a diffuse illumination with a 0° viewing angle. Detectors were silicon photo cells and the time measurement was about 1 s. Calibrations were carried out with a white ceramic plate CR-A43. Values are given in the CIE-L*a*b* colour space. These three parameters determine the colour location in colour space: L* indicates lightness (0 = absolute black, 100 = absolute white; a* and b* are the chromaticity coordinates. $+a$* is the red direction, $-a$* is the green direction; $+b$* is the yellow direction and $-b$* is the blue direction.

Colour measurements were carried out on the top face of cylindrical cores of each material (diameter 33 mm and length 70 mm).

Coloured thin sections

Thin sections were made after impregnation under vacuum of the stones by an epoxy resin stained in blue. This allows display of the porous network.

SEM images

Rock fragments, salt efflorescences and thin sections were studied by scanning electron microscopy (SEM Hitachi TM-1000 Table Top) with an energy-dispersive X-ray spectrometer (Swifted-TM Energy Dispersive XRay (EDX). The samples were introduced in the microscope without any coating, but maintained on the specimen stage by double-sided adhesive carbon tape. The accelerating voltage was 15 kV for imaging and EDX analysis. The working distance was 6 mm. All images were acquired in the back-scattered electron mode.

XRD and XRF

Salt efflorescence and debris of construction materials were collected and their mineralogical content was identified using X-ray powder diffraction (Rigaku Co. Ltd.; Ultima III). The operating conditions were X-ray target of CuKα, tube voltage of 40 kV and tube current of 40 mA, scan speed of 2.00°/min and 2/3°–0.3 mm–2/3° slits. Chemical analysis was performed using energy dispersive type of X-ray fluorescence analysis (Jeol Co. Ltd. JSX-3220).

Petrophysics

Porosity

Water total porosity of samples (P) was measured according to NF EN 1936 B 10 503 Standards.

Mercury porosimetry (P_c) was also measured on samples of 1 cm cubes with a Micromeretics AutoPore IV 9500. This apparatus quantifies the total porosity and the pore access radius distribution of the material. According to the method, the pore access radius ranges from 200 (0.003 MPa) to 0.003 μm (207 MPa). Thus, pores of larger access radius like the macropores of 0.2 mm diameter are

not taken into account. This method also determines the pore threshold (r_a), which allows the biggest part of the porous network to be filled. On the curve, the pore threshold is at the intersection of the two tangents at the top of the curve (Katz and Thompson 1986). Spreading of the curve can be defined by the scatter coefficient (C_d) calculated from a ratio of injection pressures (Wardlaw et al. 1988; Remy 1993):

$$C_d = \frac{P_{80} - P_{20}}{P_{50}} \quad (1)$$

where P_{80}, P_{50} and P_{20} are the injection pressures corresponding, respectively, to the filling of 80, 50 and 20% of the porous network. As one injection pressure corresponds to one pore radius, the scatter coefficient corresponds also to a pore radius ratio. If $C_d < 1$, the pore distribution is concentrated around one pore radius and the pore threshold value is significant. If $C_d > 1$, the pore distribution is spread. It means that the porous network is partitioned in several domains of different pore sizes (Remy 1993).

Capillary kinetics

The capillary kinetics of building materials is characterised according to the prEN1925:1999 European Standard. The bottom of the dry samples is placed in water in a tub where relative humidity is kept constant at nearly 100% to avoid drying. The weight increase per surface unit (dW/S) and the capillary height (L, wet fringe, which is measured by the naked eye) are recorded at regular intervals.

Most inorganic building materials obey the linear law of Washburn as:

$$\frac{dW}{S} = C_1\sqrt{t} + W_0 \quad (2)$$

and

$$dL = C_2\sqrt{t} + L_0 \quad (3)$$

with W_0 a small positive intercept and L_0 the height of water in the tub.

The data of weight and fringe height are plotted against the square root of time. The slope of the first curve (2) is called the C_1 coefficient (g m^{-2} s$^{-1/2}$) and is relative to the weight increase of the sample. At the end of this first linear part, the value of weight increase indicates the capillary saturation (volume of porosity invaded by water capillary absorption S_c). Next to this point, saturation of the porous network is slower with a weaker incline. This corresponds to the filling of the trapped porosity by diffusion of air through water. There is more or less trapped porosity depending on the pore distribution and on the nature of fluids used. The slope of the second curve (3), relative to the migration of the wet zone, corresponds to the C_2 coefficient (m s$^{-1/2}$).

Capillarity measurements were carried out on the same samples used for the colorimetry measurements.

Results

Petrography

Colorimetry

In the CIE L*a*b system, the three materials are easily distinguished (Fig. 5), although they have a very similar luminance (L* between 69 and 74). All three materials have positive a* and b* chromaticity values, which means that they are in the yellow–red domain. The Sinemurian stone has the lowest (a* = 1.45 and b* = 10.17) and the Bajocian has the highest values (a* = 4.39 and b* = 27.52). The reconstituted stone has intermediate values (a* = 2.60 and b* = 20.05) between the two natural stones.

Coloured thin sections

Sinemurian limestone from the Luxembourg formation in Orval is shown in Fig. 6

Elements: In this microfacies, the elements are detrital quartz grains or calcitic bioclasts. Quartz grains are dominant in the low cementation layers (Fig. 6a, b), less abundant in the layers with carbonate cement and almost absent in diagenetic recrystallisation areas or cracks with calcite fillings (Fig. 6f). Bioclasts are well preserved and easily recognisable, but frequently recrystallised in spar calcite (Fig. 6a, c). They correspond to echinoderm ossicles and bivalvia shell clasts. Oolites are sometimes observed in well-cemented and partially bioclastic layers.

Binding phase: The abundance of carbonate cement (spar calcite/sparite) varies quickly and in large proportion, as do the length and size of elements. A unique sample may show different microfacies (Fig. 6g), for example: sand with low cementation and few carbonate elements (Fig. 6e), sandy limestone with echinoderm ossicles, shells and few oolites (Fig. 6h).

Porosity: Due to cementation variations, the macroporosity observed using optical microscopy varies largely and quickly (Fig. 6g). The sandy layers show low cementation and high intergranular macroporosity (coloured in blue). In the other microfacies, the sandy bioclastic limestone is very well cemented and shows numerous recrystallisation features in spar calcite. In this case, the closure of the intergranular macroporosity is complete and elements are sometimes also recrystallised in sparite. The porosity of the bioclastic sandy limestone is very low and only shows

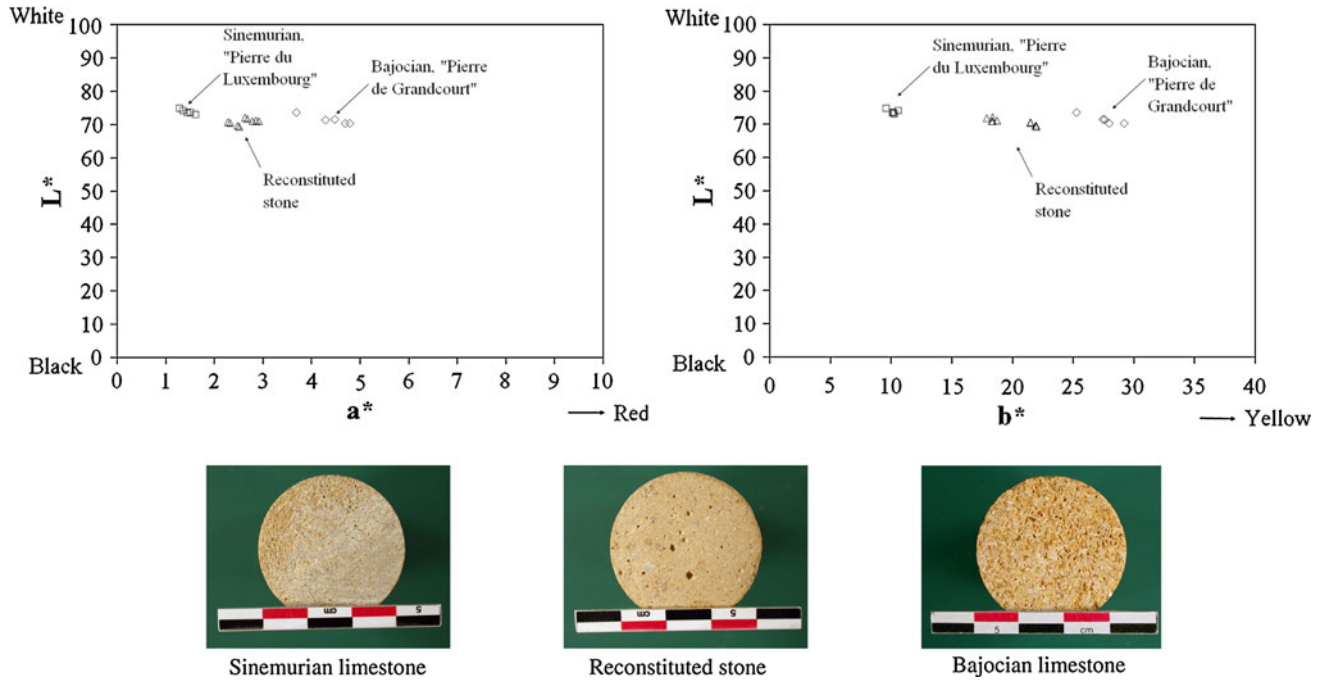

Fig. 5 Colorimetry results of Orval materials expressed in the CIE L**a***b** system

some non-connected moldic macropores corresponding to dissolution of carbonate elements without secondary diagenetic cementation. For example, in Fig. 6h, a thin microcrack is clearly stained in blue (connected porosity), whereas some intergranular macropores are not (non-connected porosity).

This microfacies of sandy limestone corresponds well to the building stone theoretically existing in the surroundings of the Orval Abbey. This limestone is known as "Assises de Florenville or Orval" (Sarlet and Matthys 1995), from Sinemurian (Lower Jurassic), and more so it is a part of the Luxembourg Sandstone formation (Van Den Bril and Swennen 2008).

Bajocian limestones from the Longwy formation originally used in Orval is shown in Fig. 7

Elements: This limestone does not show an oolitic facies, but a clear bioclastic mark. All elements in this microfacies are from biological origin: long and well-preserved calcitic shells and echinoderm ossicles (Fig. 7a) with sometimes Cidaridae spines (Fig. 7d). Shells mainly show a fibrous microstructure, corresponding to ostreid signature (Fig. 7b, c), some punctuated shells recognisable as brachiopod fragments are also observed. The other bioclasts are very rare debris of bryozoan colonies (Fig. 7c) or Textularidae foraminifers. The other calcitic elements correspond to spar recrystallised elements or spherical, but totally dissolved, elements (oolites; Fig. 7a, h). The detrital fraction is almost absent, quartz grains are very rare (unlike in the Sinemurian limestones), with only 10–20 grains per thin section. This microfacies is not a sandy limestone.

Binding phase: Carbonate cementation (spar calcite) is composed of two types of cements, one over the other. The first one is a palissadic cement, mainly developed around shell fragments (Fig. 7b, c) the second is a syntaxic cement, only developed around echinoderm ossicles (Fig. 7d, e).

Porosity: In the shell-dominated main microfacies, the residual macroporosity is important, with large intergranular pores, sometimes over several millimetres long (Fig. 7c). The porosity is very well connected. Cements developed around the few echinoderm ossicles spread in the facies are not abundant enough to close the intergranular porosity. In the minority areas, where echinoderm ossicles are numerous, syntaxic spar cements are close together and seal the intergranular macroporosity (Fig. 7g). In addition, small intragranular macropores, certainly associated with microporosity, are observed in the echinoderm fragments (Fig. 7f), or in the middle of the recrystallised or partially dissolved grains (Fig. 7h). Sometimes a moldic macroporosity is observed, especially with ghosts of spherical grains or bioclasts, for which only the micritisation envelopes remain.

Other minor diagenetic phases have little impact on porosity and are more or less developed according to the considered layer:

– A light compaction phase, characterised by some cracks into grains and cements (Fig. 7e) or by pression/dissolution joints. Intergranular macroporosity and large shells are not compacted.

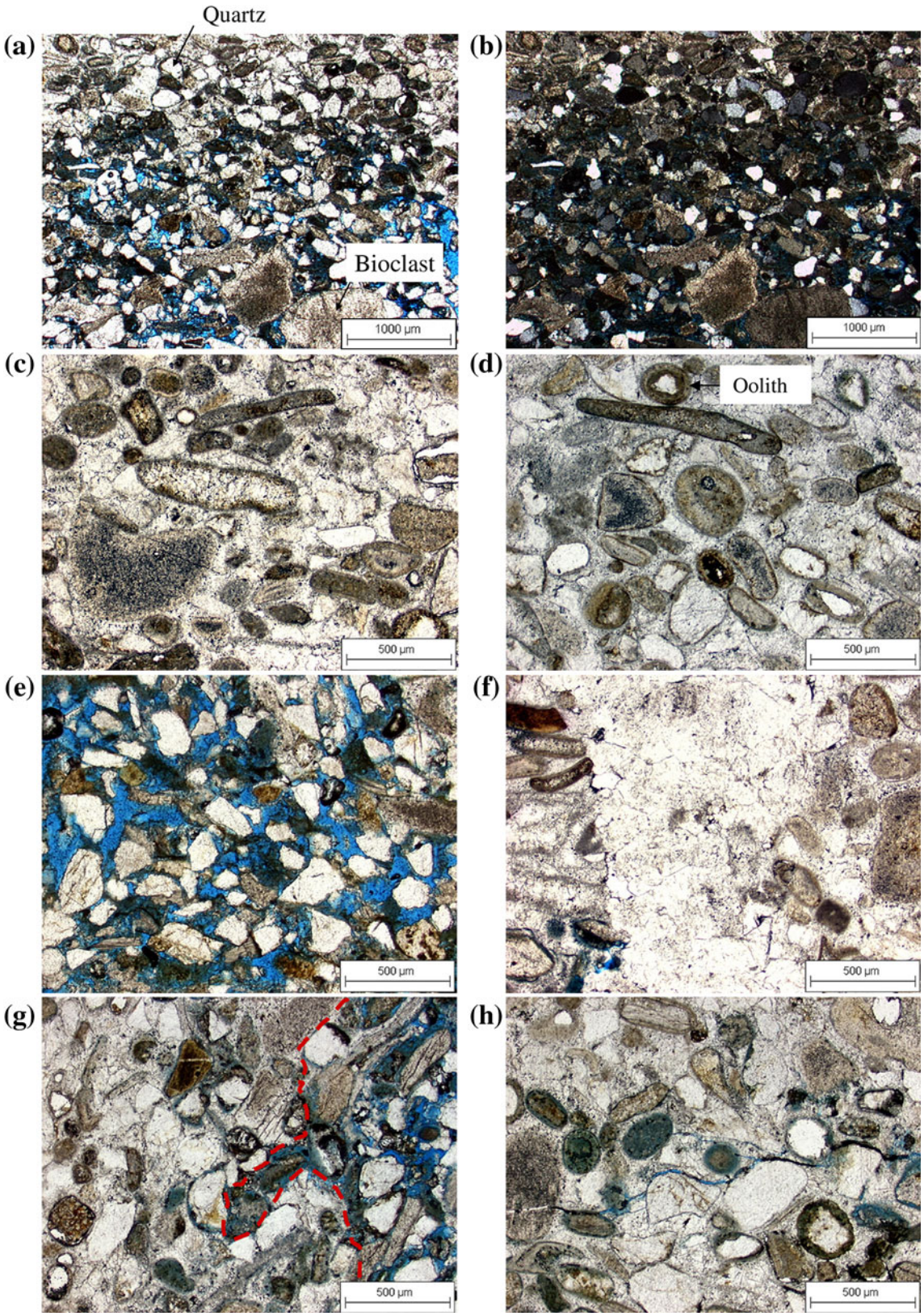

Fig. 6 *Blue*-coloured thin sections of Sinemurian limestone forming the substratum in Orval in plane polarised light except (**b**) in cross polarised light

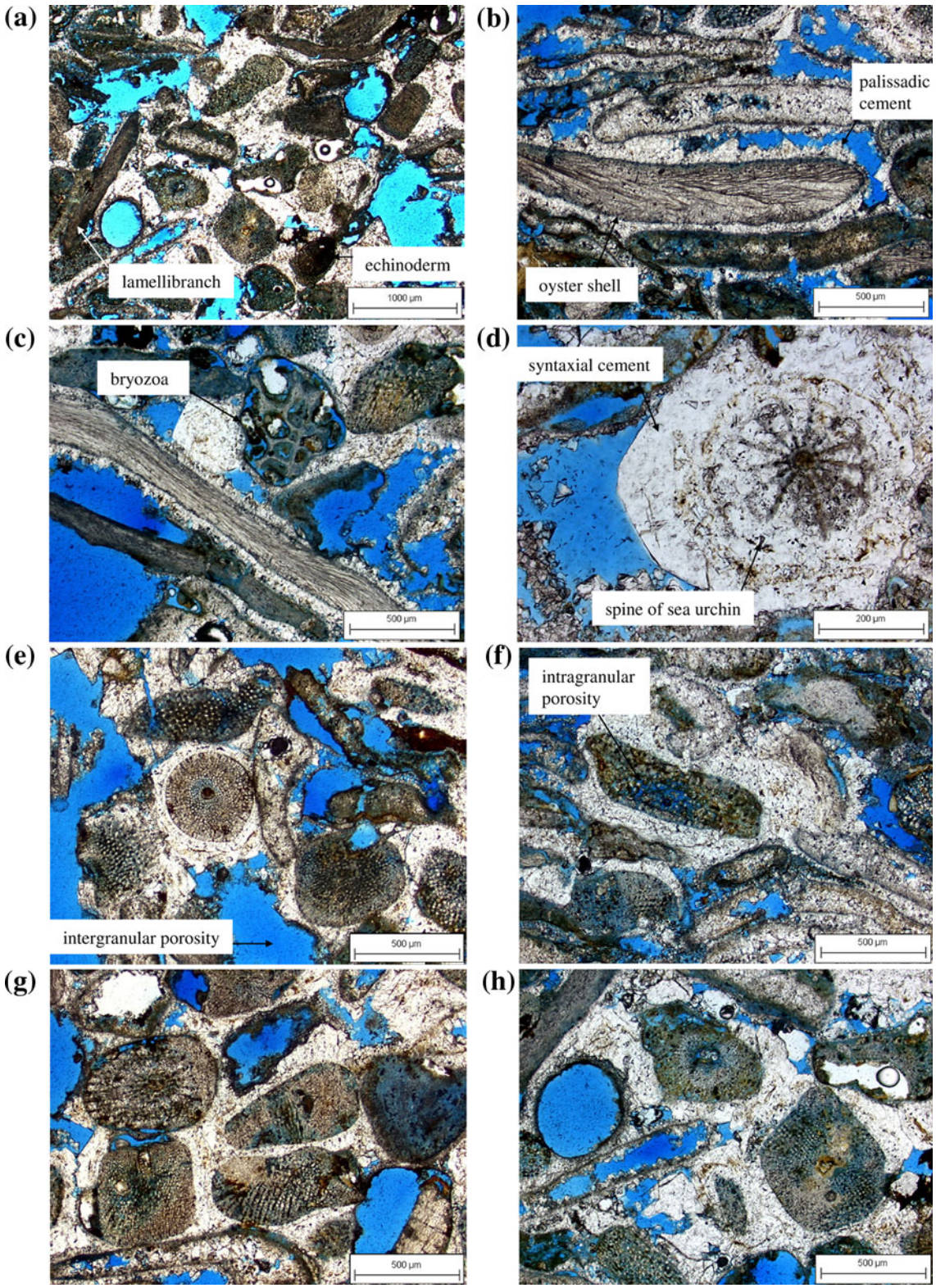

Fig. 7 *Blue*-coloured thin sections of Bajocian limestone originally used in the Orval Abbey in polarised light

– A late dissolution stage, in which the irregular diagenetic feature may affect all cements, including the syntaxic spar cement, but to a limited extent.
– Iron oxide deposits or crystallisations—in the microfacies, numerous small accumulations of iron oxides are observed. They are localised on the macropore

peripheries, on all the other diagenetic features or inside the recrystallised or partially dissolved grains. They cause the red or russet colour of the limestone and contribute to the fame of these building stones.

Reconstituted stone made in Orval in the early twentieth century is shown in Fig. 8

Elements: The reconstituted stone is a heterogeneous material mainly composed of calcareous and siliceous lithoclasts of millimetric to centimetric size and quartz grains (200–300 μm; Fig. 8a–c). Among the calcareous clasts, bivalve shell, bryozoan and echinoderm fragments are present. Among the siliceous clasts, quartz grains around 200 μm are dominant together with less abundant bioclasts.

Non-contiguous angular amorphous grains are also present. Those grains either present a homogenous light-brown colour or a radial structure, with a transparent core and a light-brown periphery (Fig. 8d). Their size ranges from 10 to 100 μm. Their abundance varies widely between different zones of a thin section.

Binding phase: In non-coloured thin sections, the fine-grained matrix appears brown coloured and is rich in very fine-grained opaque minerals (Fig. 8d). The ratio of elements to the binding phase is highly variable.

Porosity: In coloured thin sections, microporosity is revealed by a diffuse blue colour in the matrix (Fig. 8e). This feature is not systematic (Fig. 8b). Round pores corresponding to the bubbles that are visible macroscopically,

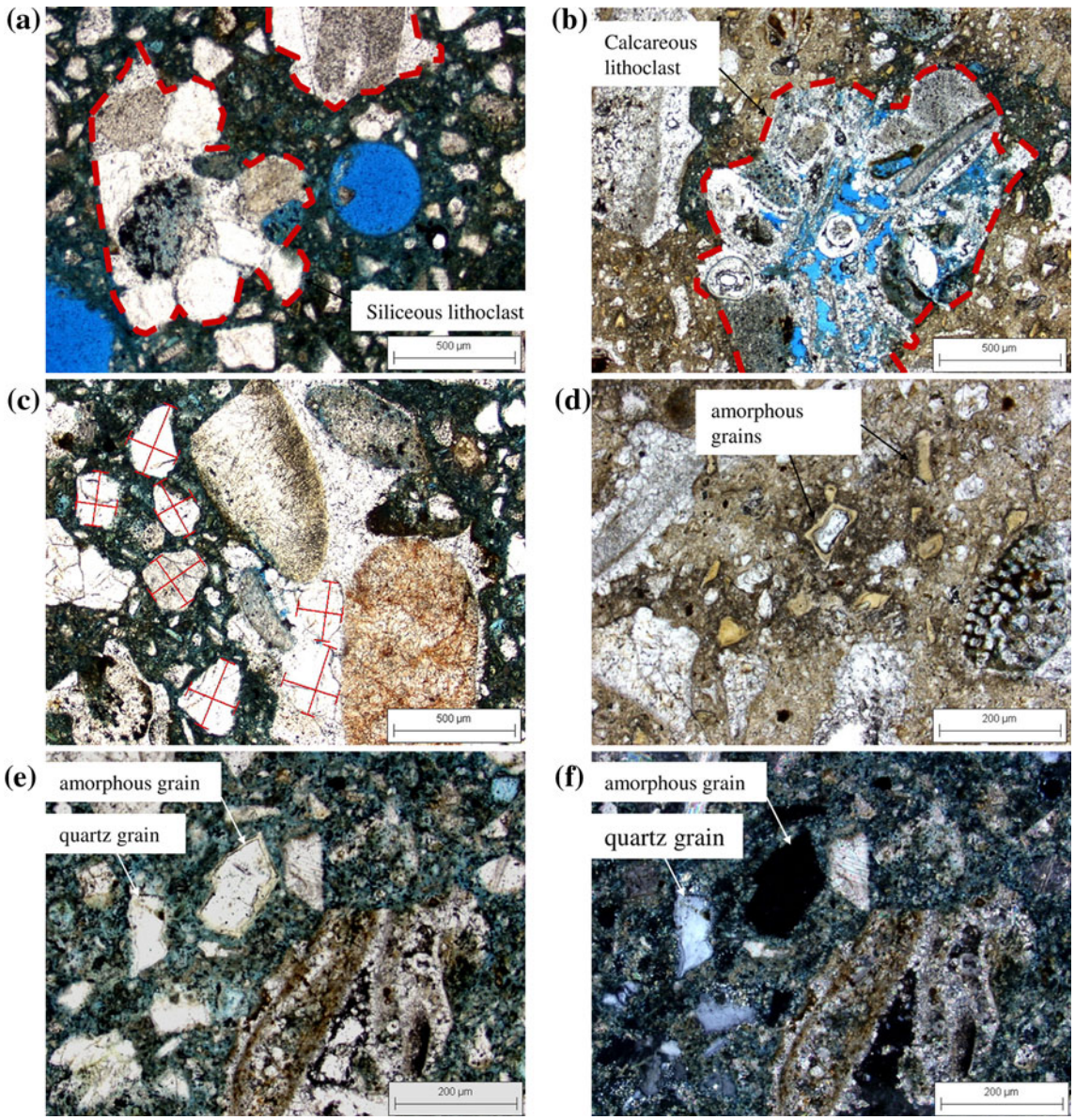

Fig. 8 *Blue*-coloured thin sections of reconstituted stone in plane polarised light

up to a few millimetres in diameter, are also present. They can be distinguished from the moldic pores present in the natural stones (Fig. 7a) by the absence of parietal coating.

Macroporosity within the calcareous lithoclasts is also present (Fig. 8b).

SEM images

Thin sections The observation of thin sections of Bajocian and Sinumerian limestones under SEM did not reveal additional features compared to the observation under petrographic optical microscope (images not shown).

The observation of thin sections of reconstituted stone provided additional information about the amorphous grains that were characterised under optical microscope. The zoned pattern was confirmed (Fig. 9a, b). An innermost zone that appeared very bright (zone A) had the most diverse chemical composition (Table 1): 50–60% Ca, 25–30% Si, 5–10% Al, 2–5% of each Mg, K and S. Several zones surround this inner part: a dark and homogeneous zone (zone B), rich in Si and Ca (40–50%) with 5–10% of K; a fibrous and bright zone (zone C) surrounding the previous one with a clear chemical contrast (90–95% Ca and 5–10% Si); the outermost part, 2 µm thick (zone D) comprising pore space and crystalline matter having a composition intermediate between B and C.

Some clusters of 50–100 µm could be distinguished in the matrix. Their chemical analyses by EDX indicated that silicon (20–60%) and calcium (20–70%) were the major components with variable percentages of iron, aluminium, potassium, sulphur and titanium (Fig. 9c, d).

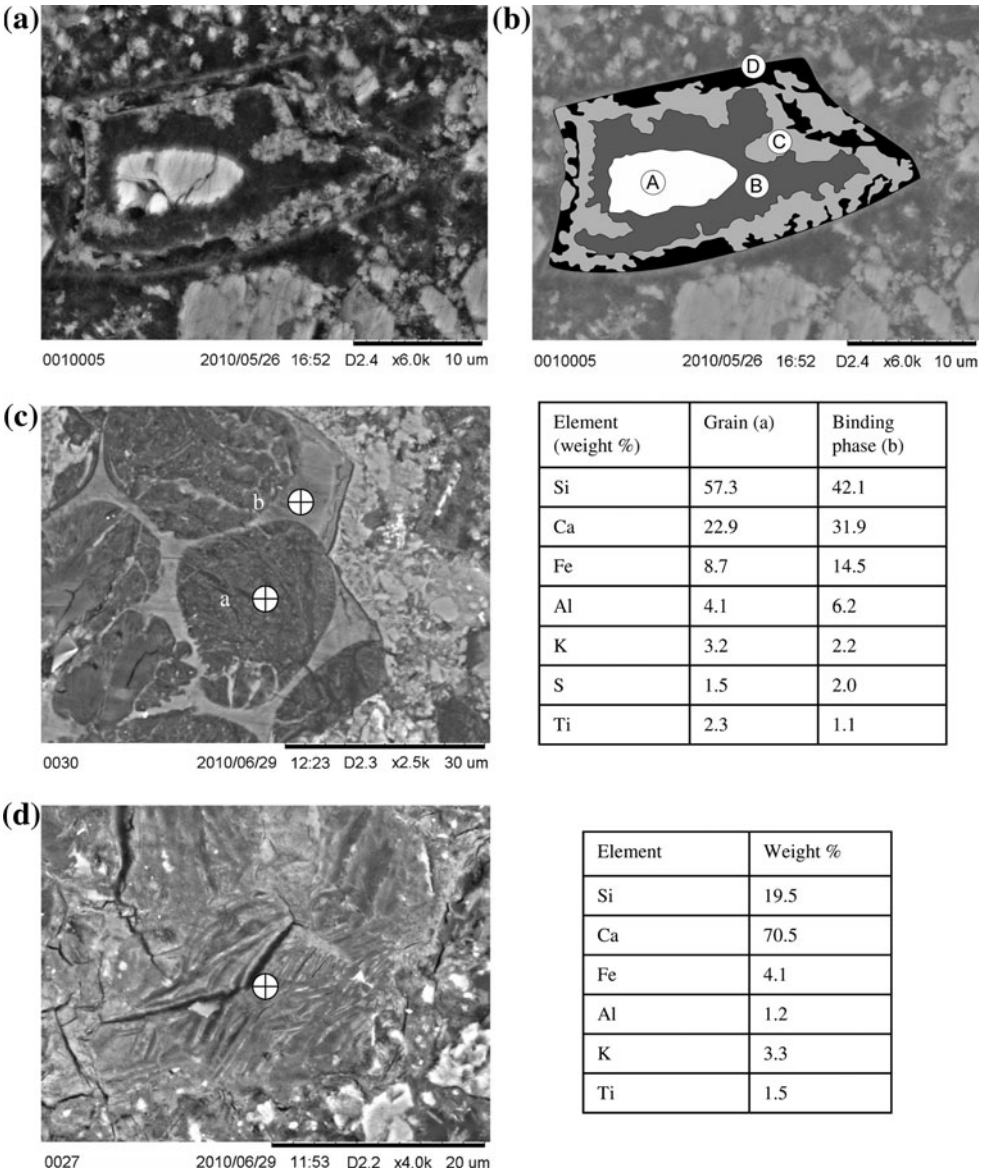

Element (weight %)	Grain (a)	Binding phase (b)
Si	57.3	42.1
Ca	22.9	31.9
Fe	8.7	14.5
Al	4.1	6.2
K	3.2	2.2
S	1.5	2.0
Ti	2.3	1.1

Element	Weight %
Si	19.5
Ca	70.5
Fe	4.1
Al	1.2
K	3.3
Ti	1.5

Fig. 9 SEM images on thin sections of a reconstituted stone. **a**, **b** Zoned amorphous grain; **c** cluster of rounded grains and EDX analyses; **d** nested grain and corresponding composition by EDX

Salt efflorescences and flaking debris are mostly constituted of minerals smaller than 10 μm and with no particular shape (Fig. 10a). In a few occasions, minerals with a typical shape and/or chemical composition could be identified: quartz *β* (bipyramidal crystals, Fig. 10b) and needle-shaped sodium and calcium sulphates (5–10 μm in length, <1 μm in diameter; Fig. 10b, c).

Table 1 EDX results on different zones of a grain composing the reconstituted stone viewed on SEM (Fig. 9a, b)

Weight %	Mg	Al	Si	S	K	Ca
Zone A: white heart	2–5	5–10	25–30	2–5	2–5	50–60
Zone B: massive crystals	–	–	40–50	–	5–10	40–50
Zone C: fibrous crystals	–	–	5–10	–		90–95
Zone D: fibrous crystals + pores	–	–	20–25	–	5–10	50–70

XRD and XRF

The results are shown in Tables 2 and 3. The dominant minerals in the reconstituted stone are calcite and quartz (approximately 45% of both CaO and SiO_2). The only oxides totalling more than 1% are Fe_2O_3 (2.88%) and Al_2O_3 (2.79%). The dominant minerals in the efflorescences are thenardite ($NaSO_4$), calcite and feldspar.

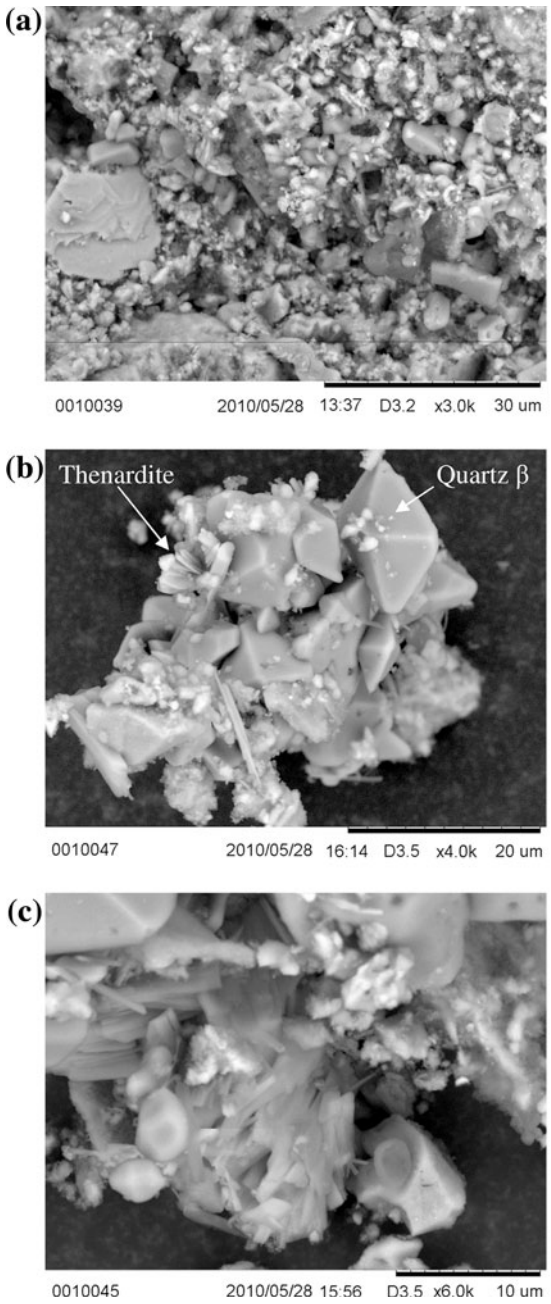

Element	Weight %
Al	8.3
Si	14.3
P	2.0
S	3.0
K	1.7
Ca	70.8

Element	Weight %
Na	31.4
Al	2.0
Si	2.4
S	61.7
Ca	2.5

Element	Weight %
Si	1.8
S	33.9
Ca	64.3

Fig. 10 SEM images of salt efflorescences at different scales and corresponding EDX composition

Table 2 Rock forming minerals and salts detected by XRD

Sample	Reconstituted stone	Efflorescence
Gypsum	–	–
Calcite	++	+
Quartz	++	–
Feldspar	–	+
Thenardite	–	+++

Petrophysics

The results are shown in Table 4.

Sinemurian limestone from the Luxembourg formation

The Sinemurian limestone has a low total porosity ($P = 7.6 \pm 0.2\%$ and $P_c = 6.6\%$). The cumulative mercury intrusion curve shows a spread distribution of pore access radii. The dispersion coefficient ($C_d = 3.4$) confirms that there is no dominant pore access radius. Only on the incremental curve does a peak appear at 0.1 μm (Fig. 11). Porosity <0.1 μm ($P_{m0.1}$) is 2.2% and porosity <5 μm (P_{m5}) is 5.3%.

The capillary coefficients are low ($C_1 = 7.3 \pm 1.2$ g m^{-2} s$^{-1/2}$ and $C_2 = 0.011 \pm 0.003$ m s$^{-1/2}$). The capillary saturation, which is the ratio of the porosity invaded at the end of capillary absorption to the total porosity, is low ($S_c = 55.3 \pm 4.7\%$).

Bajocian limestones from the Longwy formation

The Bajocian limestone has a high total porosity ($P = 31.1 \pm 0.7\%$ and $P_c = 30.0\%$). The cumulative intrusion curve shows two steep increases. Those increases correspond to two peaks that appear on the incremental curve at 0.5 and 12 μm. The dispersion coefficient ($C_d = 5.8$) is very high, owing to the presence of two marked peaks for macro- and microporosity: the porosity <0.1 μm ($P_{m0.1}$) is 1.0% and the porosity <5 μm (P_{m5}) is 6.9%. The capillary coefficients are the highest of the three materials of the Orval Abbey ($C_1 = 96.6 \pm 5.7$ g m^{-2} s$^{-1/2}$ and $C_2 = 0.053 \pm 0.001$ m s$^{-1/2}$). The capillary saturation also has the highest value ($S_c = 63.1 \pm 2.5\%$).

Reconstituted stone

Reconstituted stone has a high total porosity ($P = 28.2 \pm 0.9\%$ and $P_c = 25.4\%$), slightly lower than that of the Bajocian limestone. The cumulative intrusion curve shows one steep increase that is confirmed by the incremental curve (threshold at 0.12 μm) and by the low value of the dispersion coefficient ($C_d = 1.5$). The porosity <0.1 μm ($P_{m0.1}$) is 12.9% and the porosity <5 μm (P_{m5}) is 24.2%. The capillary coefficients are slightly lower than those of the Bajocian limestone ($C_1 = 93.2 \pm 7.2$ g m^{-2} s$^{-1/2}$ and $C_2 = 0.041 \pm 0.0006$ m s$^{-1/2}$ and $S_c = 51.1 \pm 0.6\%$).

Discussion

Three main types of building materials can be found in the Orval Abbey:

– A Sinemurian limestone quarried from the substratum of the abbey (Luxembourg formation) and a Bajocian limestone quarried from the Longwy formation about 20 km southeast of the abbey. These two natural limestones are typical building materials in this part of the sedimentary Paris Basin. They have been used since

Table 3 XRF results on the reconstituted stone

Element	MgO	Al_2O_3	SiO_2	P_2O_5	SO_3	K_2O	CaO	TiO_2	Cr_2O_3	MnO	Fe_2O_3	ZnO	SrO	ZrO_2	Total
Weight%	0.68	2.79	45.46	0.83	0.43	0.93	45.20	0.32	0.12	0.03	2.88	0.08	0.20	0.04	99.99

Table 4 Porosity and capillary kinetics of Orval building materials

		Sinemurian limestone	Bajocian limestone	Reconstituted stone
Water porosimetry	Total porosity P (%)	7.6 ± 0.2	31.1 ± 0.7	28.2 ± 0.9
	Total porosity P_c (%)	6.6	30.0	25.4
Mercury porosimetry	Pore thresholds R_a (μm)	0.1	0.5 and 12	0.12
	Dispersion coefficient C_d	3.4	5.8	1.5
Capillary absorption	Weight increase per surface unit C_1 (g m^{-2} s$^{-1/2}$)	7.3 ± 1.2	96.6 ± 5.7	93.2 ± 7.2
	Wet fringe migration C_2 (m s$^{-1/2}$)	0.011 ± 0.003	0.053 ± 0.001	0.041 ± 0.006
	Capillary saturation S_c (%)	55.3 ± 4.7	63.1 ± 2.5	51.1 ± 0.6

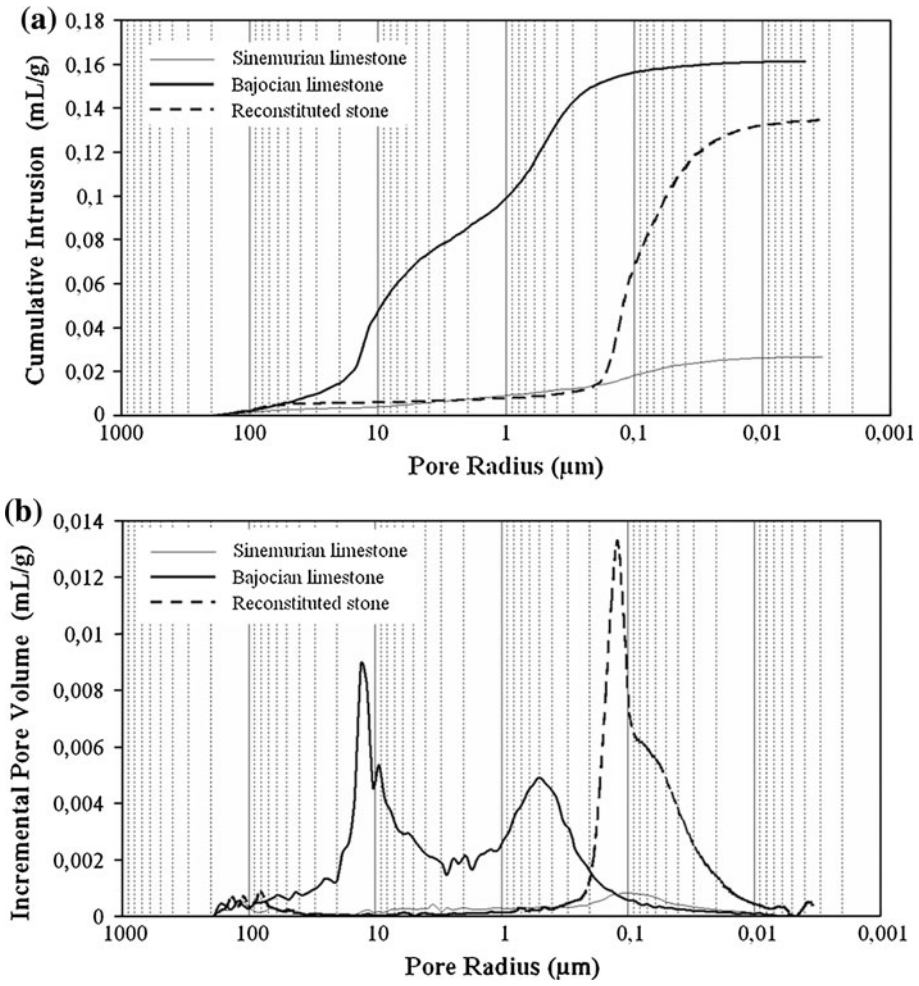

Fig. 11 Pore access distribution of Orval building materials measured by mercury porosimetry: **a** cumulative intrusion (ml/g) and **b** incremental pore volume (ml/g)

the first building of the abbey. Most of the quarries can be located and their use for the building of Orval is well documented.

– Reconstituted stone made and used in the abbey from 1932 to the end of the rebuilding of the abbey in 1948. The making process and composition are hardly known, as if making such a material was not considered to be noble. The only information known for sure from historical sources is that this reconstituted stone was made by different craftsmen at the site of the abbey using rock debris found in the ruins and Bajocian limestone debris of blocks quarried in the Pas-Bayard quarry and cut in the abbey.

The microscopic observations and petrophysical characterisations revealed that the Sinemurian limestone has a marked detrital signature. It contains a majority of quartz grains, close to 200 µm in diameter and is highly cemented and has a low porosity (7.6%). This stone, although available locally, is difficult to cut and is used mostly as rubble stone. The Bajocian limestone is richer in bioclastic elements (echinoderm and bivalve debris) and has much higher porosity (31.1%). This stone is easier to cut and thus used as freestone. The reconstituted stone is composed of various-sized lithoclasts of the previous stones and individual quartz grains, all bound by cement. Its total porosity (28.2%) is slightly lower than that of the Bajocian stone, but much higher than that of the Sinemurian stone. The colorimetry measurements showed that the reconstituted stone has a colour very close to that of the natural stones. In this aspect, the objective of making a cheaper, but similar in porosity and colour, replacement for the quarry materials was achieved.

Different elements were observed within the cement. Amorphous grains from 10 to 100 µm with a zoned pattern and a chemical composition corresponding to calcium silicate, containing sulphur and aluminium, were interpreted as clinker grains that had partially reacted (Fig. 9a). Clusters of rounded grains were found showing a nested pattern and a chemical composition close to that of the classically described phases of alite (C3S), belite (C2S), ferrite (C4AF) or aluminate (C3A), but with a higher proportion of sulphur (Fig. 9b; Taylor 1997).

As with all building materials, the stones making up the abbey are submitted to meteorological factors and weathering according to their position in the monument (for example, exposed or sheltered zones, zones prone to capillary rise, orientation…). The setting of the Orval Abbey in a swampy valley surrounded by forests is favourable to biological colonisation of the stones. It is, however, striking that only the parts of the building made of reconstituted stone show salt weathering. In those parts, salt efflorescences are systematic in capillary rise zones and zones supplied with water (Fig. 2). Although they are submitted to the same exposure conditions, the natural stones of Bajocian and Sinemurian are devoid of salt efflorescences and flaking.

Microscopic and chemical characterisation of efflorescences and flaking debris showed that they were mostly thenardite ($NaSO_4$). This salt is one of the most common ones that can be found in salt-weathered concrete (Thaulow and Sahu 2004). Thenardite is an anhydrous mineral, but can change phase to the decahydrate sulphate mirabilite. This spontaneous transition is controlled by the temperature and accompanied by an important volume expansion (314%, Tsui et al. 2003), thus inducing crystal pressure. Apart from the visual impairment of the building, thenardite formation thus causes mechanical damage to the building stones (Rodriguez-Navarro and Doehne 1999), as observed in the abbey (Fig. 3b, c).

The chemical elements composing the salt efflorescences and flaking debris are probably not of atmospheric origin because the abbey is located far from urban areas, but more certainly from the soil or from the stones themselves. The microscopic observations of salt efflorescences and flaking debris revealed quartz β associated with thenardite (Fig. 10b). This high-temperature (>573°C) polymorph of silica was probably formed during the clinker firing process. Its association with thenardite hints that the origin of salts is within the cement itself.

Before discussing the details of the porous network, it should be noted that the mercury-estimated porosity does not take the pores bigger than 200 μm into account. This is particularly important for the reconstituted stone, in which millimetric-sized bubbles are visible to the naked eye and on Figs. 3a, 5 and 8a. This can account for the difference of up to 3% between the water and mercury method results for the reconstituted stone. Although the total porosity of the reconstituted stone is similar to that of the Bajocian stone, the details of the pore access distribution stone shows that in that aspect the reconstituted stone is very different from that of the natural stones. Excluding the bubbles, the pore size distribution of the reconstituted stone is centred on 0.1 μm, as is the pore size distribution of the Sinemurian limestone. This may correspond to the diffuse porosity observed on the coloured thin sections in the cement (Fig. 8a, e). This distribution contrasts with the bimodal distribution of the Bajocian stone, with peaks of macropores at about 12 μm (corresponding to moldic porosity and partial dissolution of spar cement in the matrix) and micropores at about 0.5 μm (intragranular porosity corresponding to partial dissolution in bioclasts).

The pore size distribution was used to calculate the salt susceptibility indices (SSI) for the three stones, following Yu and Oguchi (2009). This calculation takes the values of P_c, $P_{m0.1}$ and P_{m5} as inputs to define *SSI* as follows:

$$\mathrm{SSI} = (I_{Pc} + I_{Pm0.1})\frac{P_{m5}}{P_c} \quad (4)$$

In this calculation, each parameter accounts for a specific aspect of salt susceptibility: P_c is a rough indicator of salt susceptibility, refined by P_{m5} that controls the salt uptake, and $P_{m0.1}$ that has a critical influence on salt crystallisation damage. The results are shown in Table 5. According to the *SSI* values and the nomenclature of Yu and Oguchi (2009), the Sinemurian stone is *highly salt resistant* (SSI = 1.6), the Bajocian stone is *salt prone* (SSI = 4.0) and the reconstituted stone is *highly salt prone* (SSI = 13.6). The porous network of the reconstituted stone is thus more susceptible to salt weathering than the natural stones it was made of.

Given the properties of the three materials and their behaviour on the monument, efficient conservation strategies of the Orval Abbey will have to focus on the reconstituted stone rather than on the natural stones. Further analyses of the cement and historical investigation of the manufacturing process will be necessary. In particular, one will have to confirm that the source of the salts is within the reconstituted stone itself and get a more precise view of the quantities involved. Monitoring stations have recently been set up in different salt-weathered parts of the abbey. To determine when salt crystallises and if the mineralogy of salts changes over time, temperature and relative humidity are recorded and salts are collected. Laboratory experiments of salt weathering are planned. Field monitoring and

Table 5 Salt susceptibility parameters calculated after Yu and Oguchi (2009)

	Sinemurian limestone	Bajocian limestone	Reconstituted stone
Total porosity P_c (%)	6.6	30.0	25.4
Index of connected porosity I_{Pc}	3	6	7
Porosity < 0.1 μm $P_{m0.1}$ (%)	2.2	1.0	12.9
Index of microporosity $I_{Pm0.1}$	2	1	7
Porosity < 5 μm P_{m5} (%)	5.3	6.9	24.2
Salt susceptibility index (SSI)	4.0	1.6	13.3

laboratory results would help evaluate if desalination would be appropriate or if other remediation methods would apply.

Conclusion

In a historical context when natural stone was in short supply, the building of the modern Orval Abbey employed reconstituted stone made from debris of natural stones and cement. This enabled reproducing the visual aspect of natural stone. Even though most of its properties were roughly equivalent to those of the natural freestone, the making process probably induced the presence of sodium sulphate and of a porous network highly susceptible to salt weathering. In the case of the Orval Abbey, conservation strategies will ironically have to focus on the material that was used most recently.

Acknowledgments This work has been partly funded by InterregIV European grant (project Hybriprotech), co-financed by FEDER, Région Champagne-Ardenne, Conseil général des Ardennes, Conseil général de la Marne and Région Wallonne (CTS, MG, GF, SE and BK) and by JSPS (CTO). The authors would like to thank: Brother Xavier, steward of the abbey for allowing the authors to work on this beautiful monument; Eric Hance, the present architect of the Orval Abbey, and Pierre Maîtrejean, member of Aurea Vallis et Villare association, for their precious information about Orval history; Jean-Didier Mertz of Laboratoire de Recherche des Monuments Historique for having carried out mercury porosimetry; Xavier Drothière for his help in the preparation of figures.

References

Benavente D, Cueto N, Martínez-Martínez J, García del Cura MA, Cañaveras JC (2007) The influence of petrophysical properties on the salt weathering of porous building rocks. Environ Geol 52:215–224

Brigaud B, Durlet C, Deconinck J-F, Vincent B, Thierry J, Trouiller A (2009a) The origin and timing of multiphase cementation in carbonates: impact of regional scale geodynamic events on the middle jurassic limestones diagenesis (Paris Basin, France). Sediment Geol 222(3–4):161–180

Brigaud B, Durlet C, Deconinck J-F, Vincent B, Pucéat E, Thierry J, Trouiller A (2009b) Facies and climate/environmental changes recorded on a carbonate ramp: a sedimentological and geochemical approach on Middle Jurassic carbonates (Paris Basin, France). Sediment Geol 222(3–4):181–206

Gomez-Heras M, Smith BJ, Viles HA (2010) Oxford stone revisited: causes and consequences of diversity in building limestone used in the historic centre of Oxford, England. In: Prikryl R, Torok A (eds) Natural stone resources for historical monuments. Geological Society, London, Special Publications 333:101–110

Goudie AS, Parker AG (1998) Experimental simulation of rapid rock block disintegration by sodium chloride in a foggy coastal desert. J Arid Environ 40:347–355

Katz AJ, Thompson AH (1986) Quantitative prediction of permeability in porous rock. Phys Rev 34(7):8179–8181

Mosquera MJ, Silva B, Prieto B, Ruiz-Herrera E (2006) Addition of cement to lime-based mortars: effect on pore structure and vapor transport. Cement Concrete Res 36(9):1635–1642

Remy JM (1993) Influence de la structure du milieu poreux carbonaté sur les transferts d'eau et les changements de phase eau-glace. Application à la durabilité au gel de roches calcaires de Lorraine, PhD thesis, Institut National Polytechnique de Lorraine

Rodriguez-Navarro C, Doehne E (1999) Salt weathering: influence of evaporation rate, supersaturation and crystallisation pattern. Earth Surf Proc Land 24:191–209

Rozenbaum O, Barbanson L, Muller F, Bruand A (2008) Significance of a combined approach for replacement stones in the heritage buildings' conservation frame. CR Geosci 340:255–345

Ruiz-Agudo E, Mees F, Jacobs P, Rodriguez-Navarro C (2007) The role of saline solution properties on porous limestone salt weathering by magnesium and sodium sulfates. Environ Geol 52:269–281

Sarlet D, Matthys A (1995) Le Patrimoine Monumental de la Belgique-Wallonie, Province du Luxembourg, arrondissement de Virton. P. Mardaga Editor, p 508

Taylor HFW (1997) Cement chemistry. Thomas Telford, London

Thaulow N, Sahu S (2004) Mechanism of concrete deterioration due to salt crystallization. Mater Charact 53:123–127

Tsui N, Flatt RJ, Scherer GW (2003) Crystallization damage by sodium sulphate. J Cult Herit 4(2):109–115

Van Den Bril K, Swennen R (2008) Sedimentological control on carbonate cementation in the Luxembourg Sandstone Formation. Geol Belg 12(1–2):3–23

Wardlaw NC, Mckellar M, Li Y (1988) Pore and throat size distributions determined by mercury porosimetry and by direct observation. Carbonates Evaporites 3(1):1–15

Yu S, Oguchi CT (2009) Role of pore size distribution in salt uptake, damage, and predicting salt susceptibility of eight types of Japanese building stones. Eng Geol (in press)